

ASI

Carbon – Science and Technology

ISSN 0974 – 0546

http://www.applied-science-innovations.com

ARTICLE Received : 08/09/2014, Accepted:17/9/2014

Investigations on thermal properties, stress and deformation of Al/SiC metal matrix composite based on finite element method

K. A. Ramesh Kumar[1], K. Balamurugan[2], S. Arungalai Vendan[3], J. Bensam Raj[4]

[1]Department of Mechanical Engineering, Nandha College of Technology, Erode
[2] Department of Mechanical Engineering, Institute of Road and Transport Technology, Erode
[3]School of Electrical Engineering (SELECT), VIT University, Vellore
[4]The Raajas Engineering College, Tirunelveli

AlSiC is a metal matrix composite which comprises of aluminium matrix with silicon carbide particles. It is characterized by high thermal conductivity (180-200 W/m K), and its thermal expansion are attuned to match other important materials that finds enormous demand in industrial sectors. Although its application is very common, the physics behind the Al-SiC formation, functionality and behaviors are intricate owing to the temperature gradient of hundreds of degrees, over the volume, occurring on a time scale of a few seconds, involving multiple phases. In this study, various physical, metallurgical and numerical aspects such as equation of continuum for thermal, stress and deformation using finite element (FE) matrix formulation, temperature dependent material properties, are analyzed. Modelling and simulation studies of Al/SiC composites are a preliminary attempt to view this research work from computational point of view.

Keywords: AlSiC, FEA, Deformation, Stress, Composite

1. INTRODUCTION

1.1 Overview of Finite Element Analysis (FEA)

Finite Element Method (FEM) is most established and extensively employed tool for solving the non-linear partial differential equations which arise in the mathematical modelling of various processes. The procedural steps in the application of typical finite element method are illustrated in Figure (1). A discrete finite element model is generated from a variation or weak form of the mathematical model.

1.2 Application of Finite Element Analysis to Al –Si Composites:

The analytical study of any physical phenomenon engrosses two key tasks viz., the mathematical formulation of the physical process and the numerical analysis of the modelled process of system. The mathematical formulation of a physical process necessitates good background knowledge in the allied subjects and more frequently, in using mathematical tools. The finite element method is a potential numerical technique formulated to evaluate multifarious physical processes. The method is characterized by three features (Eager 1990).

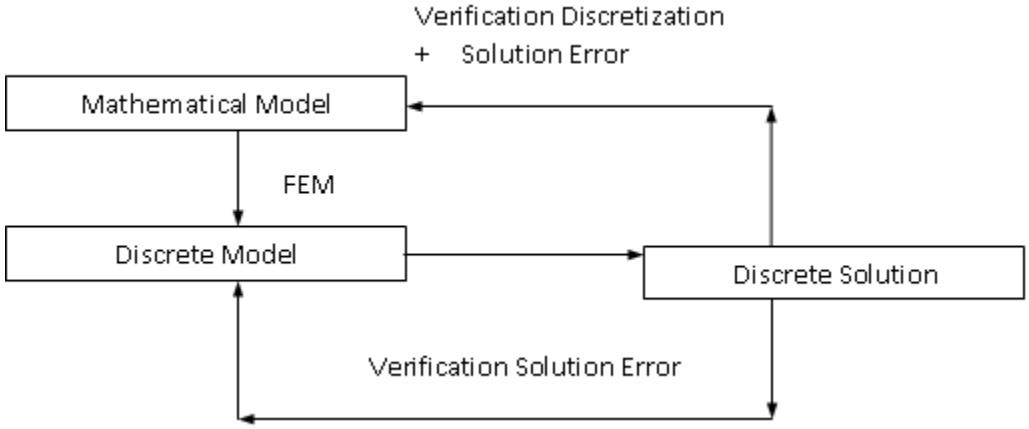

Figure (1): Finite Element Procedures

1. The domain of the problem is represented by a collection of simple sub domains called finite elements. The collection of finite elements is called the finite element mesh.
2. Over each finite element, the physical process is represented using appropriate functions of desired type, and algebraic equations relating physical quantities at selective points, called nodes.
3. The element equations are assembled using continuity and / or balance of physical quantities.

When a metal matrix composite (MMC) is cooled down from the fabrication or annealing temperature to room temperature, the mismatch of the thermal expansion coefficients of the matrix and reinforcement induces residual stresses in the composite. In this preliminary/ basic research study on FEM applied to MMC, a thermomechanical model describing these processes is presented considering that the reinforcement component has thermo-elastic behavior and that the matrix material exhibits a thermo-elasto-viscoplastic behavior. The model is implemented with a finite element method algorithm and the resulting code is used to perform numerical simulations and calculate thermally induced residual stress fields and deformation parameters in MMCs. The purpose of this research study is to present a three-dimensional finite element algorithm dedicated to the numerical calculation of thermally induced residual stresses in metal matrix composite materials. The mechanical model considers the reinforcement component to behave thermoelastically and the matrix material to have thermoelasto-viscoplastic behavior. The developed code is tested with some numerical examples concerning SiC reinforcement in an aluminium matrix.

2.0 MATHEMATICAL MODELLING AND ALGORITHMS:

The continumm kinematics approach used to describe the thermal and mechanical behavior of metal matrix composites is briefly presented in this section.

2.1 Associative Modeling:

When multiphase materials are subjected to changes in temperature, residual stress fields are induced. These are generally generated by the differences in the **Coefficients of Thermal Expansion** (CTE) of the constituent materials. The behavior of materials under these conditions has been investigated by many researchers often using experimental techniques (Ledbetter et al 1987, Fang et al 2000, Fernandez et al 2004 & Bruno et al 2004).

2.2 Continumm Kinematics:

The idea is to resolve the current configuration of the material, Ct, starting from the reference configuration on a previous instant, C_0. Let P be a material point in the continuous medium O and p and x the position vectors of this material point in the configurations C_0 and Ct, respectively, then

$$P = \bar{p}(x,t) \tag{1}$$

$$x = \bar{x}(p,t) \tag{2}$$

$$x = p + u(p,t) \tag{3}$$

where u (p,t) represents the displacement of the material point P between the configurations C_0 and Ct. The gradient F of the point transformation x can be defined as:

$$F(p,t) = F = \frac{\partial}{\partial p}\bar{x}(p,t) = I + \frac{\partial}{\partial p}u(p,t), \tag{4}$$

where I is the second order identiry tensor. The velocity field associated with this transformation is

$$\bar{x}(p,t) = \bar{x}(\bar{p}(x,t),t) = \frac{\partial}{\partial p}\bar{x}(p,t) \tag{5}$$

to which corresponds the velocity gradient L, defined as

$$L(x,t) = grad[v(x,t)] = \frac{\partial}{\partial x}\mathrm{v(x,t)} = \frac{\partial}{\partial p}\bar{x}(p,t)\frac{\partial}{\partial x}\bar{p}(x,t) \tag{6}$$

where grad is the gradient operator relative to x, keeping t constant.

2.3 Material Behavior:

The target of this text is to model the development of residual stresses in metal matrix composites (MMC). These stress fields can occur, for instance, from the cooling down stage that is imposed on the MMC during the manufacturing process. Let T be the cooling rate that is considered constant. Besides, it will be assumed that the temperature field T(t) is homogeneous within the material. Its evolution can then be described by

$$T(t) = T_0 + Tt \tag{7}$$

where T_0 is the initial temperature value, at time instant $t = t_0$. The material is considered to be stress free at $t = t_0$, which is a rational consideration due to the manufacturing temperatures of most metal matrix composites (Shen et al 1995). In industrial processes involving the cooling down of two or more distinct materials (e.g. reinforcement and matrix) it is imperative to discern each behavior model. This distinction will be made by unfolding the melting (decomposition) temperature of each material (T^m) and the process temperature. This relation is designated by homologous temperature (T^h) and can be defined as

$$T^h = \frac{T}{T^m} \tag{8}$$

2.4 Constitutive Modelling of the Reinforcement:

The maximum temperature levels reached during the manufacturing processes of most MMCs are much lower than the decomposition temperature of the reinforcement materials, thus the homologous temperature is often $T^h < 1$. It is reasonable to consider that the reinforcement material exhibits thermoelastic behavior. As a consequence, the following hypotheses are assumed (Suery et al 1993) (i) elastic strains are small (ii) elastic behavior is isotropic and (iii) the influence of plastic strain on the elastic constants can be neglected. The reinforcement behavior can then be described by Hooke's hyperelastic law (Hughes 1994)

$$\sigma = C_R^e : D^e \tag{9}$$

The thermal part of the strain rate tensor is $D^t = \alpha_R$ TI and α_R is the thermal expansion coefficient of the reinforcement. Combining and manipulating (Kolhe 1996) it can be determined that

$$\sigma = 2\mu_R D^{te} + \left[\left(k_R - \frac{2}{3}\mu_R\right) trace(D^{te}) - 3k_R\alpha_R T\right] I,$$

with $$k_R = \lambda_R + \frac{2}{3}\mu_R \tag{10}$$

2.5 Modeling of the Matrix:

The maximum temperature reached during the manufacturing process of the MMC is often the same order of magnitude as the melting temperature of the matrix material. This reveals that the matrix homologous temperature is $T^h \sim 1$. This emphasizes that the material behavior is both temperature and strain rate dependent. The proposed model will allow the modelling of the phenomena such as (i) the effects of strain rate and temperature (ii) static and dynamic recovery and recrystallisation processes (iii) internal damage and its evolution and (iv) crystalline structure and its evolution.

The important equation governing the temperature dependent strain inducing aspect in the MMC is presented here and the other derivation and interrelated equations and formulas have been evaded owing to copious discussions and procedures already available in several literatures.

$$h(\bar{\sigma}, S, T) = h_0 \left|1 - \frac{s}{s^*}\right|^a sgn\left(1 - \frac{s}{s^*}\right) \tag{11}$$

with a > 1, the equation may be further modified based on the equations derived while arriving at the solution which are not presented here owing to the abundance in its availability in literature.

$$s = \bar{\varepsilon}^P \left[h_0 \left|1 - \frac{s}{s^*}\right|^a sgn\left(1 - \frac{s}{s^*}\right)\right] \tag{12}$$

where h_0 is the hardening rate and s* is a saturation value for the scalar variable s, associated with a determined temperature and strain rate, such that

$$s^* = \bar{s}\left[\frac{\bar{\varepsilon}^P}{A} exp\left(\frac{Q}{R_g T}\right)\right]^n \quad (13)$$

The constants h_0, a, $\bar{s}$ and n are once more material parameters.

3.0 PROCEDURE FOR FINITE ELEMENT ANALYSIS

The general finite element modeling procedure consists of the following steps Lindgren (2001) as shown in Figure (2).

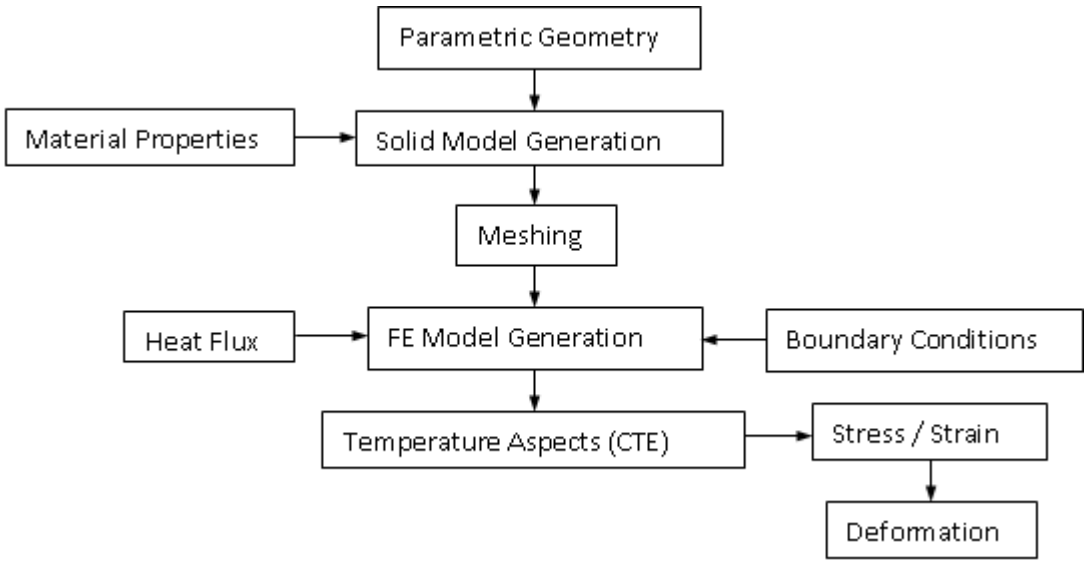

Figure (2): Procedure for finite element analysis

4.0 SIMULATION MODEL:

Metal matrix composites are analyzed using finite element modeling and image processing technique. In their study a comparative finite element study of two dimensional and three dimensional microstructure based model of a composite reinforced with ceramic particles was formulated (Fatma Ayari1 et al 2012). Hillol Joardar et al (2012) investigated the deformation behavior of solid cylinders of an aluminum metal matrix composites subjected to axial stress. The friction factor at die hard interface is assessed with ring compression and its non uniform deformation pattern is examined. FEM analysis is carried out for SiC in Al Si-doped aluminium) matrix, that takes into account both thermal and stress enhancers. In this research study, a simulation model based on Kang et al (2005) is adopted. A perfect simple cubic system, which is negligible on defects such as pores is assumed. FCC models based structures are also considered. FEM computations are employed to investigate displacement due to thermal expansion. Generally, MMC is composed of a metal matrix and reinforcing particles. Available literatures (Zhao et al 2007 & Zhang et al 2003) illustrates that the arrangement of reinforcement material plays an important role in changing of CTE.

Figure (3) shows the simulation model of the SiC with simple cubic arrangement in Al, respectively. Generally, computational difficulties are encountered while carrying out simulation and obtaining reasonable results based on a small single unit owing to a deficiency in interaction between reinforcement particle and matrix.

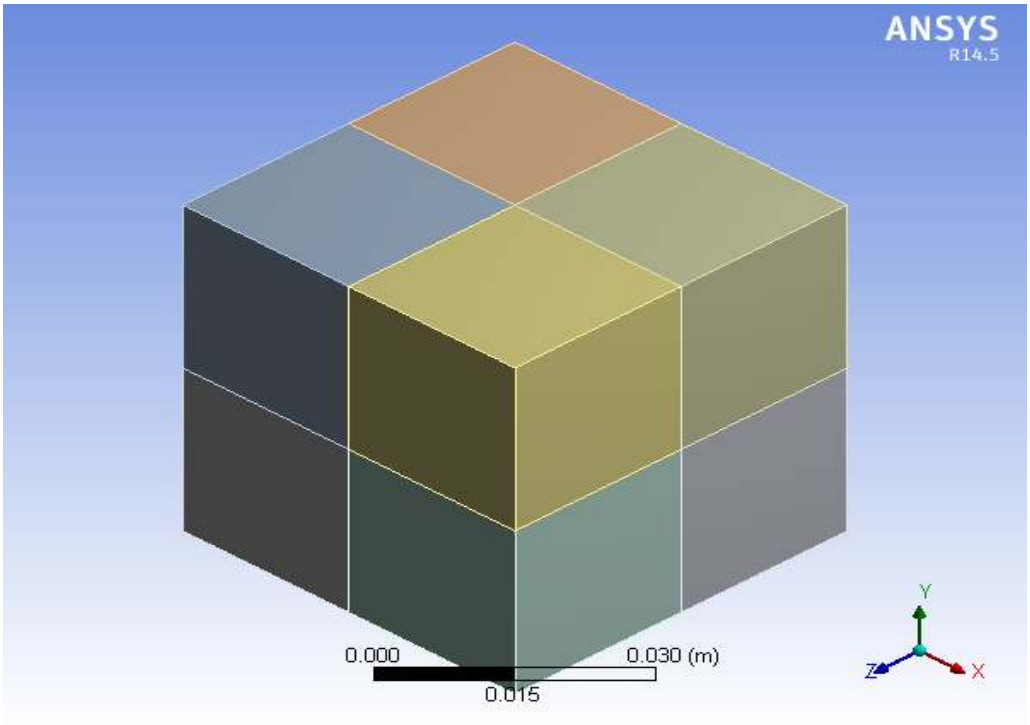

Figure (3): Al matrix with SiC particles

The adopted model is designed with Al matrix and SiC reinforcement, however, for the case where SiC volume is larger than that of the metal, MMC model can be reversed, so that the matrix is SiC and metal becomes the particle. Here, the 3-D model mesh was converted into a finite element mesh with commercially available ANSYS software package.

To find the effect of volume fraction, the Al matrix with SiC reinforcement was used to achieve 9 – 50% SiC volume fraction and the opposite case was considered to achieve 60 – 90% SiC volume fraction. To analyze the CTE, the temperature of finite element mesh was increased from initial temperature of 25 ^{0}C to 100 ^{0}C during simulation.

Table (1): Mechanical properties of Al and SiC

Material	Temperature (^{0}C)	CTE (ppm/^{0}C)	Young's Modulus (Gpa)	Yield Stress (MPa)
Al	25	19.4	79	315
	200	20.2	-	62
	300	21.0	-	24
SiC		2.72	20.8	3440

Material properties with marked reliance on temperature are used in this simulation. Al and SiC were considered as an isotropic, perfectly elastic material. The material properties are summarized in Table 1.

5.0 RESULTS AND DISCUSSION

5.1 Coefficient of Thermal Expansion Analysis

When SiC was added in Al matrix with increasing SiC volume fraction, the CTE value was decreased linearly. The fact attributing to this observation is that the result is smaller than that of Al, consequently, SiC ensues a suppressed state resulting in the difference of their CTE values. From results in Figure 4

the model conditions between simple cubic and face centred cubic are considered to have a very similar behavior due to few difference of that CTE results.

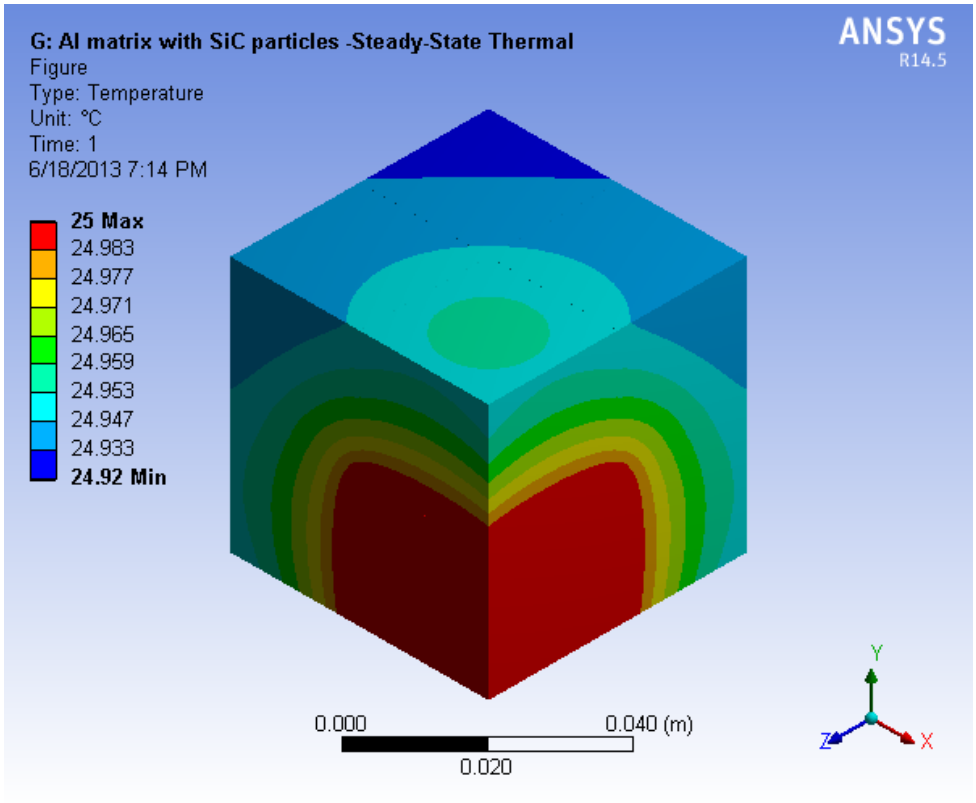

(a)

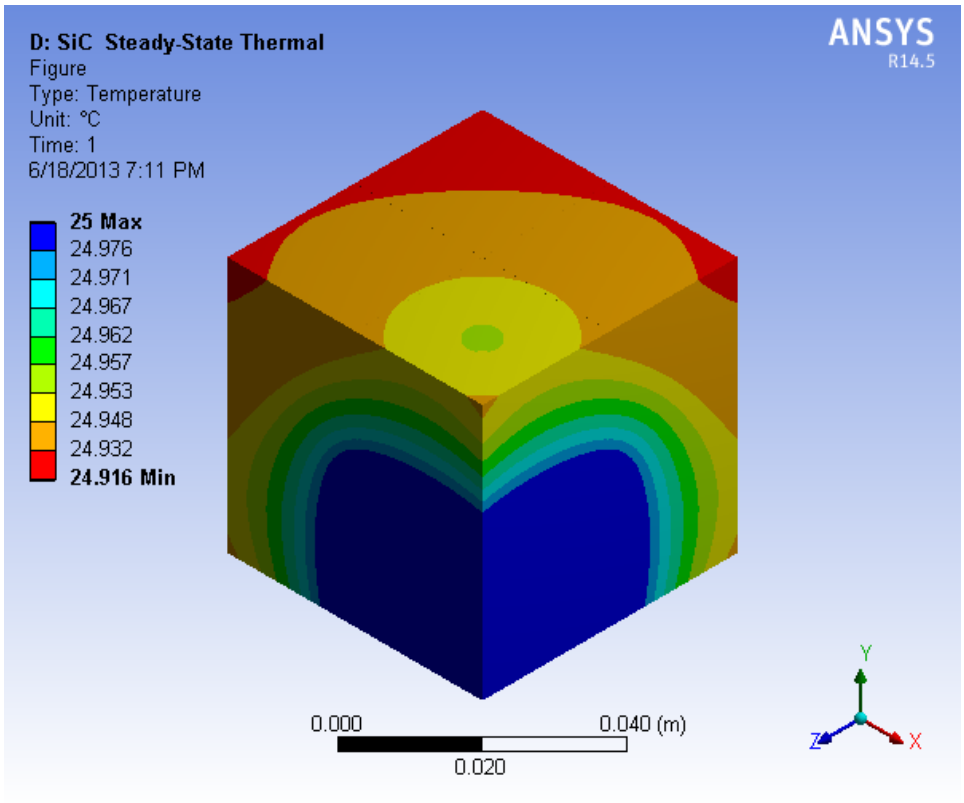

(b)

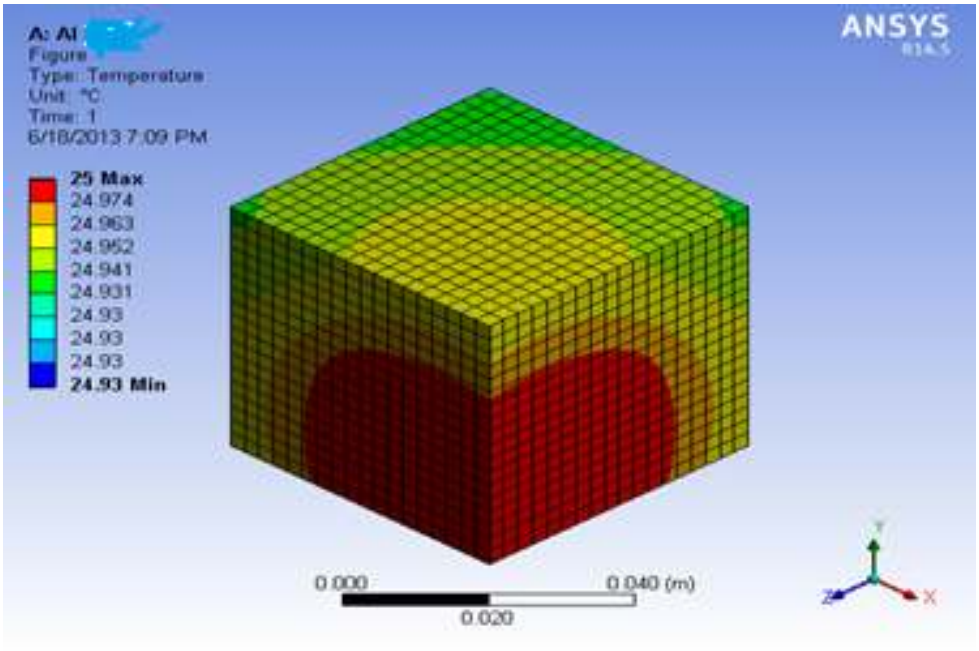

(c)

Figure (4): The method to measure the CTE of MMC. To remove the free edge effect, two more shells are calculated and CTEs of MMC were measured in core cell.

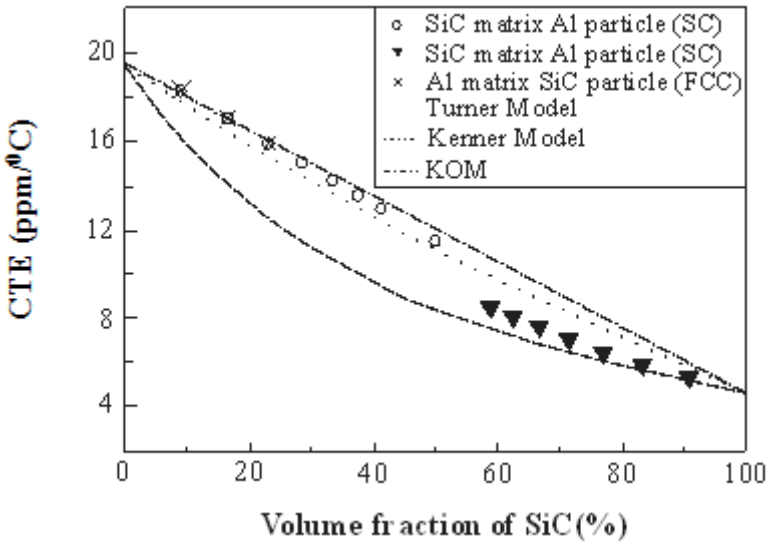

Figure (5): Calculated CTEs of MMC for simple cubic site SiC, simple cubic site Al, and face centered cubic site SiC

The CTEs of simple cubic site SiC and face centered cubic site SiC MMCs were measured almost same at the volume fraction of 9–23% and they showed promising results.

As reported earlier, the CTE of Al matrix with SiC particles becomes larger than that of the opposite case. Figure 4 reveals that the prototype results varied as a function of temperature. The left image in Figure 4 displays the simulated model with non deformed condition given at 25 ^{0}C and the right image shows the deformed model with thermal stress upto 100^{0}C.

For the opposite case of SiC matrix, when the volume fraction of SiC is above 50%, a linear decrease in the CTE was observed. The obtained tendency on computational manner tended close to the predicted from Kernal's model and Turnal's model. The bulk modulus appears to govern this model and the linearity dissapears in SiC matrix of Figure 5. Nevertheless, SiC volume fraction is, indeed, main factor contributing to the CTE of MMC.

5.2 Stress Analysis:

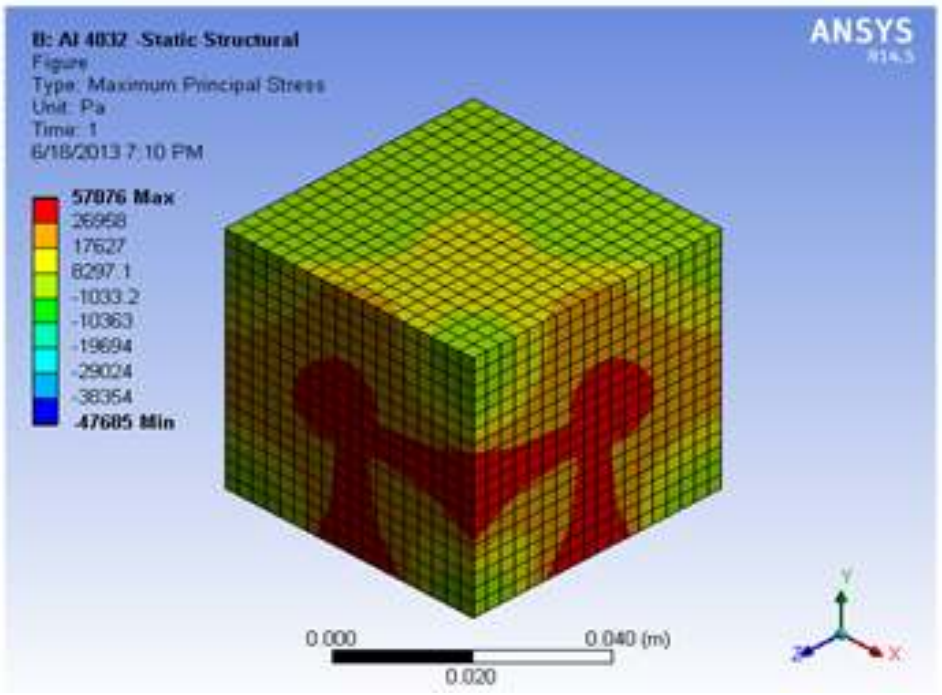

(a)

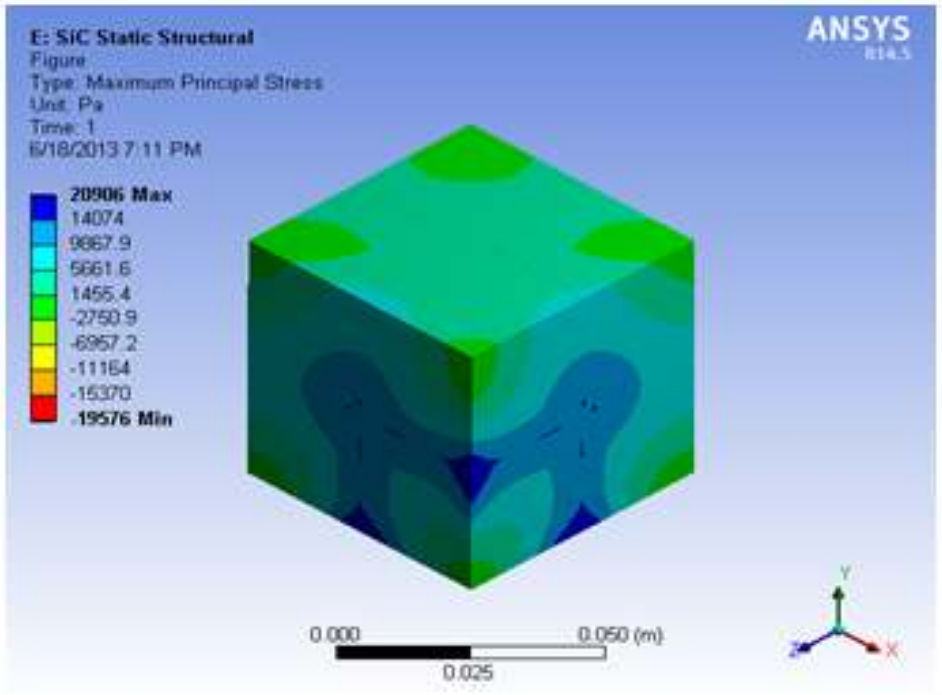

(b)

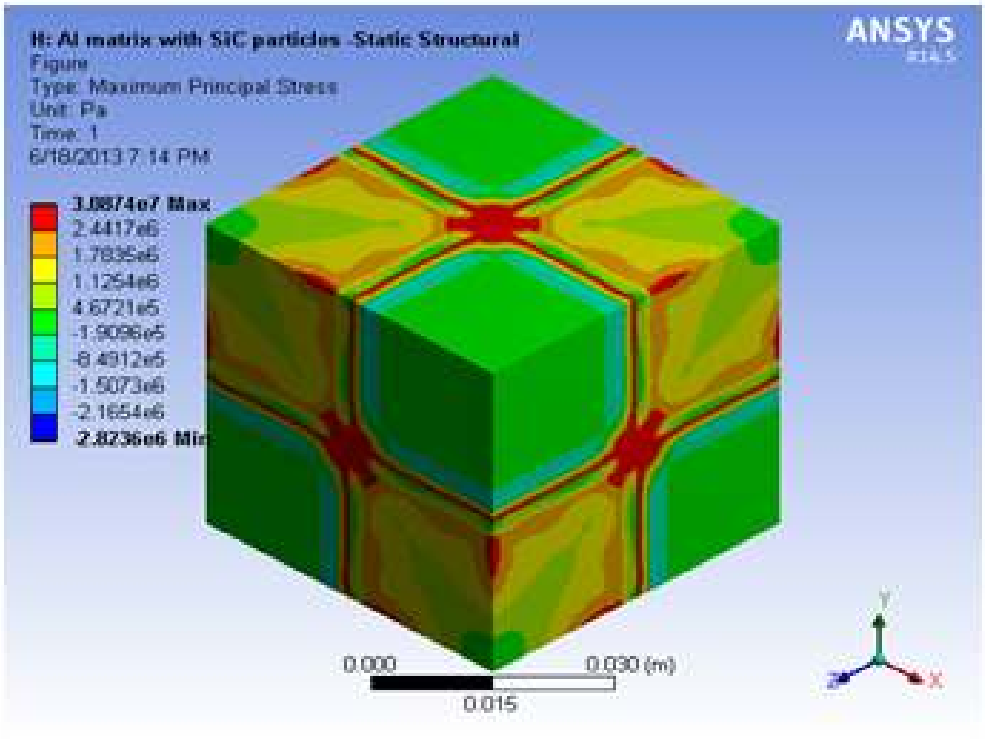

(c)

Figure (6): The stress concentration contours of thermally expanded MMC (SiC volume fraction = 30% and Δ T=75 ^{0}C (a) Al matrix, simple cubic site SiC particles, (b) SiC matrix, simple cubic site Al particles, (c) Al matrix, face centered cubic site SiC particles.

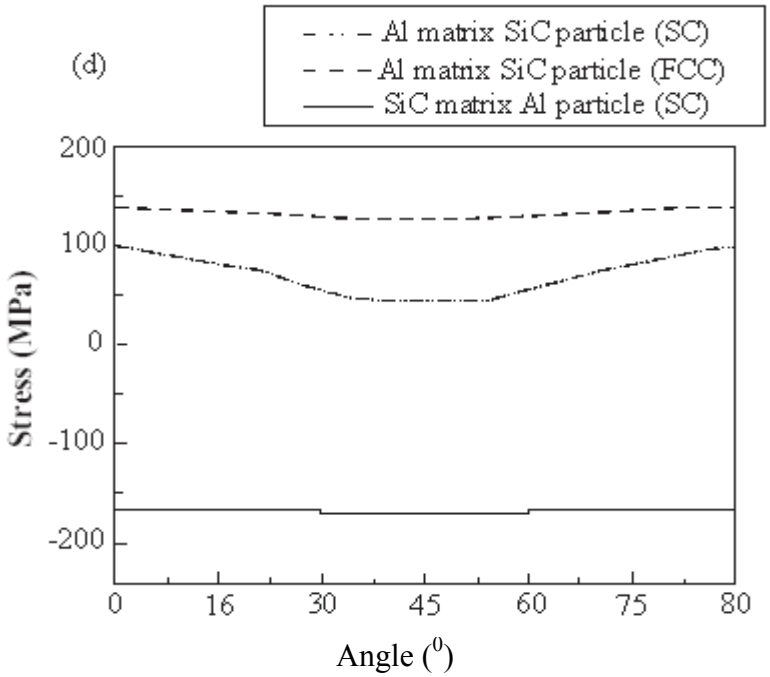

Figure (7): The principal stress for Al through the path.

Expansion and deformation occurs steadily following the heating of MMC. Thermal stress is induced by the difference of lattice constants between the matrix and the particles. Maximum principal stress on each case corresponding to a different cubic arrangement of SiC is displayed with Al matrix Figure (6a), it emphasizes that the thermal expansion induced the tensile stress at Al near the interface. Figure (6b)

displays SiC/Al matrix in simple cubic, where the stress turned to compressive stress since the linked SiC particles contracted the expansion of Al at the volume fraction of increased SiC. For Al/SiC matrix in FCC Figure (6c). The MMC of Al matrix face centered cubic site SiC particles has more tensile stress evolutions than the MMC of Al matrix simple cubic site SiC particles at same volume fraction.

Figure (7) shows the computed thermal stress results compared with Figure (6a) and Figure (6b), additionally, the measured difference between Figure (6a) and Figure (6c) is also shown in Figure (7). The reason on the difference between Figure (6a) and Figur (6c) can be explained with their arrangement including each different CTE. From this viewpoint of structure arrangement, the more packed structure, such as FCC, allows the stress to increase owing to enhanced stress field induced by surrounding atoms.

Additional consideration on the Figure (6a) and Figure (6b) were described as follows. In case of Figure (6a) the smaller CTE of SiC in heated state renders Al matrix expansion so that plus value of thermal stress were measured. On the other hands, in case of Figure (6b) Al thermal stress in Al/SiC matrix can be obtained with compressed value (i.e. minus value) because Al particles are isolated in SiC matrix even though Al has larger CTE rather than SiC matrix (Eusun Yu et al 2008). The corresponding deformations occurring in the Al-SiC material determined through FEM analysis using ANSYS is shown in Figure (8a-c).

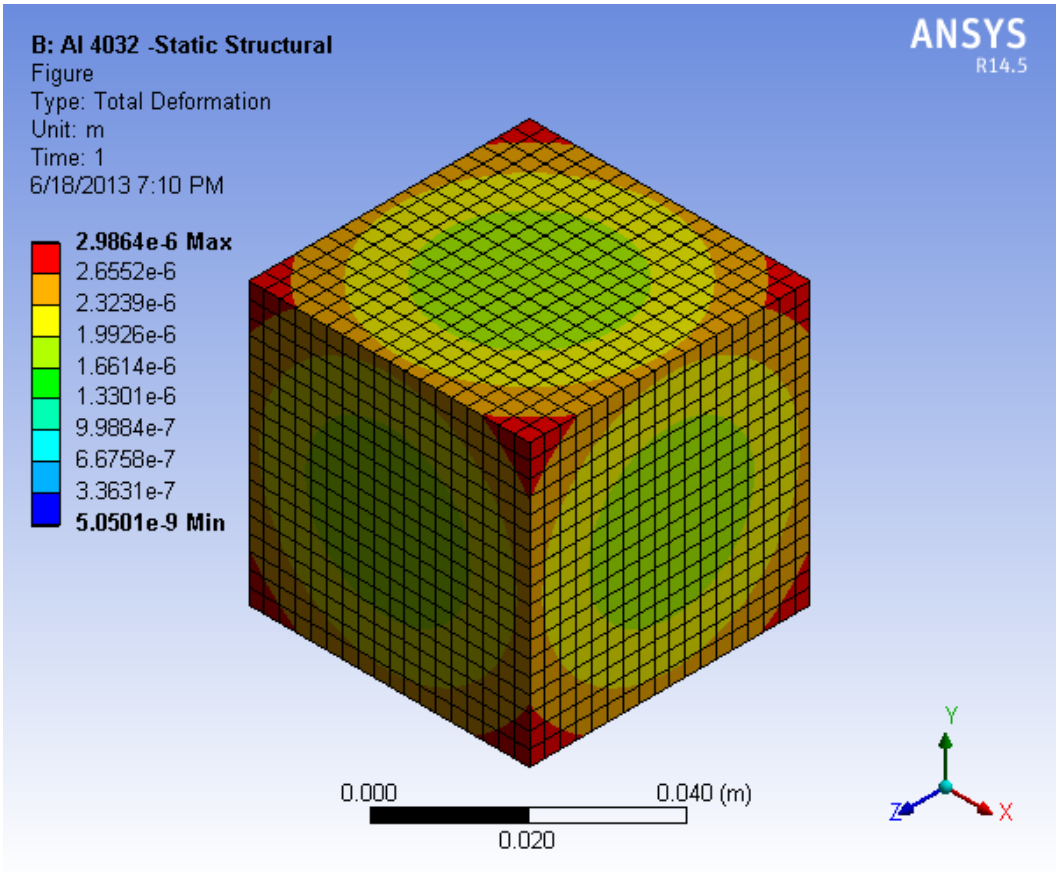

(a)

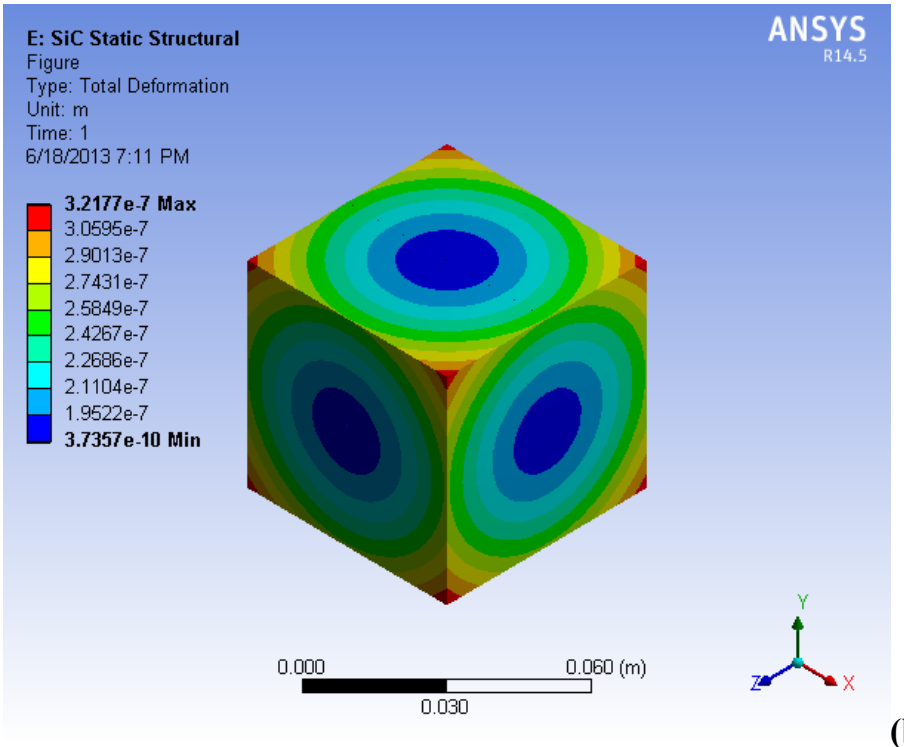

(b)

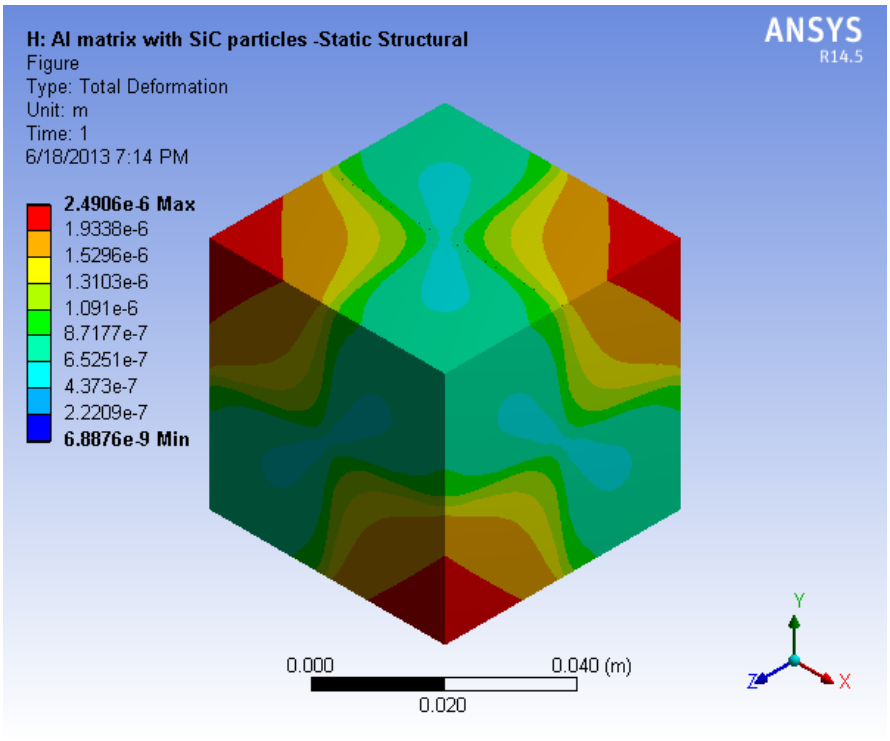

(c)

Figure (8): (a-c) Total deformations in Al-SiC Material

6 CONCLUSIONS:

In this research, preliminary attempts were made to investigate thermal properties of Al/SiC MMC over all mixing composition via FEM analysis. To calculate their coefficient of thermal expansion with FEM analysis, SC and FCC cubic system composed of Al/SiC possessing differences of structure having

MMC is adopted. The obtained results are in a good agreement with previous experimental reports. Additionally, the calculated CTE values are also confirmed with a qualitative extracted equation. This work though is not a significant breakthrough, still tries to explain little behavior of the Al/SiC composites from computational approach point of view and supports experimental outcome.

REFERENCES:

1. M. F. Ashby, *Acta Metall. Mater*. **41**, 1313 (1993).
2. N. Chandra, C.R. Ananth, *Compos. Sci. Technol.* **54**, 87 (1995).
3. S. Lemieux, S. Elomari, *J.Mater. Sci.* **33**, 4381 (1998).
4. C.Y.H. Lim, S.C. Lim, M. Gupta, *Wear,* **255**, 629 (2003).
5. S. F. Hassan, M. Gupta, *J. Mater. Sci* **37**, 2467 (2002).
6. Narasimalu Srikanth, Manoj Gupta, *Acta Mater*. **54**, 4553 (2006).
7. A. B. Pandey, B. S. Majumar and D. B. Miracle, *Acta Mater*. **49**, 405 (2001).
8. L.Z. Zhao, M.J. Zhao, X.M. Cao, C. Tian, W.P. Hu, J.S. Zhang, *Compos Sci Technol* **67**, 3404 (2007).
9. Q. Zhang, G. Wu, G. Chen, L. Jiang, B. Luan, *Compos. Part A-Appls.* **34**, 1023 (2003).
10. N. Chawla, V.V. Ganesh, B. Wunsch. *Scripta Mater.* **51**, 161 (2004).
11. (a) N. Chawla, X. Deng, D.R.M. Schnell, *Mat. Sci. Eng.* **426**, 314 (2006). (b) E. H. Kerner, *Proc Phys Soc* **69 B**, 808 (1956).
12. P. S. Turner, *J. Res. Nat. Bureau Stand.* **37**, 239 (1946).
13. C.G. Kang, J.H. Lee, S.W. Youn, J.K. Oh. *J. Mater. Process. Tech.* **166**, 173 (2005).
14. L. C. Davis, C. Andres, J. E. Allison, *Mat. Sci. Eng. A,* **249** 40 (1998).
15. ASM Handbook, Vol 2 (1991), 10th edn. ASM International.
16. Fatma Ayari, Fayza Ayari Emin Bayraktar, Chokri Ben Amar, International Journal of Computer Science Issues, Vol. 9, Issue 5, No 1, September (2012).
17. Hillol Joardar, Goutam Sutradhar, Nitai Sudar Das, Journal of Minerals and Materials Characterization and Engineering, 11, 989-994 (2012)

***